厚生労働科学研究費補助金　肝炎等克服緊急対策研究事業
C型肝炎を含む代謝関連肝がんの病態解明及び治療法の開発等に関する研究
分担研究報告書

肝細胞癌発生予後に係る代謝関連因子に関する研究

研究分担者　建石 良介　東京大学大学院医学系研究科　特任講師

研究要旨：近年増加しつつある非ウイルス性肝細胞癌の背景因子、病態、予後を特に代謝関連因子に着目して検討した。平成24年度には通院中の糖尿病および高血圧患者を対象としFibroScan®による肝硬度測定および肝脂肪量の測定を開始した。平成25年度には全国55の第3次医療機関において1991年～2010年までに診断された非B非C型肝細胞癌5633症例を収集し、階層化クラスタリングの手法を用いて5つのカテゴリーに大別した。平成26年度には、体組成の構成要素である骨格筋量、内臓脂肪量、皮下脂肪量、筋内脂肪量を測定し、肝癌治療後の予後との関係を検討した。非B非C肝癌においては、肥満・糖尿病・脂肪肝を背景とした代謝関連肝癌が大半を占めることをあらためて明らかにするとともに、これらの発生母体であるコホートを設定し、長期経過を観察するプラットフォームを確立できた。また、体重減少だけでなく筋肉量の維持・増強がこれら肝癌患者の予後向上に役立つ可能性を見出した。

A. 研究目的

近年増加傾向にある非B非C肝癌の背景には生活習慣病の影響が大きいと考えられているが、その詳細はこれまで明らかになっていない。我々は、非B非C肝細胞癌の高危険群と考えられる、肥満・糖尿病・脂肪肝を合併した集団の囲い込みと危険因子の分析、発癌後の予後改善を目指した方策の検討を目的として研究を行った。

B. 研究方法

①肝硬度測定装置であるFibroScan®に新たに肝脂肪の定量を可能にするControlled Attenuation Parameter (CAP)と呼ばれるソフトウエアを導入し、東京大学医学部附属病院消化器内科通院中の慢性肝疾患・肝硬変・肝細胞癌患者および、糖代謝内科通院中の糖尿病患者を対象に2012年2月より測定を開始した。②全国55の第3次医療機関において1991年～2010年までに診断された非B非C型肝細胞癌5633症例を収集した。そのうち、PBCや自己免疫性肝炎などの固有の慢性肝疾患を除き、データの欠損のない2166例を対象に16の臨床データを用いた階層別クラスタリングを行った。③当院で診断された肝細胞癌患者を対象に筋肉、皮下脂肪、内臓脂肪を分離して計測することによって体組成のそれぞれの構成因子が肝癌患者の予後に与える影響を検討した。

（倫理面の配慮）

本研究は文部科学省、および厚生労働省によって公表されている疫学研究に関する倫理ガイドラインに則り、東京大学医学部倫理委員会に承認を受けている（承認番号960, 2058, 3710）

C. 研究結果

①2012年11月末までに詳細なデータを入力し終えた966人について分析を行った。肝硬度の中央値6.8kPa (範囲:2.5-75kPa)、肝脂肪量(CAP)の中央値は、216dB/m(範囲100-366dB/m)であった。各々肝硬変(>15kPa)、脂肪肝(>260kPa)に該当する者の割合は、17.6%、23.4%であった。背景疾患毎に肝硬度、肝脂肪量を検討したところ、肝硬度は、B型で有意に低く、肝脂肪量は、非B非Cで有意に高いという結果であった。その後も引き続き経過観察を行っている。

②階層クラスタリングによって、対象者は、以下の5つの群に大別できた：C1 高齢男性、中等度飲酒、肝機能正常、C2 高齢男性、肥満、中等度飲酒、肝硬変、C3 比較的若年男性、大量飲酒、肝機能不良、C4 肥満男性、非飲酒、生活習慣病、C5 高齢女性、肥満、非飲酒、肝硬変。年代別の各グループの割合を検討したところ、C1とC5の増加が近年の非B非C肝癌の増加に寄与している可能性が示唆された。③骨格筋量が少ないほど、内臓/皮下脂肪面積が大きいほど、筋内脂肪量が多いほど有意に予後不良であった。低体重群に骨格筋量の少ない「サルコペニア」が多く含まれ、肥満群では、内臓脂肪、筋内脂肪が有意に多いことが判明した。

D. 考察

肝細胞癌発癌には、20年以上の長期間を要する。肝発癌の端緒である糖尿病・脂肪肝患者を囲い込み経過観察を行うことと同時に終末像である肝硬変・発癌例の詳細を検討することによって、時間的に大きく隔たった2つの病態をつなぐことができる。

E. 結論

非B非C肝細胞癌は、肥満・糖尿病・脂肪肝を背景とし、これらの病態が長期間続くことによって発生すると考えられる。近年の非B非C肝癌の増加の背景には生活習慣病の増加があり、これらを解決することが非B非C肝細胞癌の減少につながると思われる。一方、すでに肝硬変に至っている例、発癌に至っている例に関しては、減量とともに筋肉量の増強を促すことが予後の改善につながる可能性がある。

F. 健康危険情報

なし

G. 研究発表

1. 論文発表

1) Nakagawa H, Fujiwara N, Tateishi R, Arano T, Nakagomi R, Kondo M, Minami T, Sato M, Uchino K, Enooku K, Asaoka Y, Kondo Y, Shiina S, Yoshida H, Koike K. Impact of Serum Levels of Interleukin-6 and Adiponectin on All-Cause, Liver-Related, and Liver-Unrelated Mortality in Chronic Hepatitis C Patients. J Gastroenterol Hepatol 2015;30(2): 379-88.

2) Tateishi R, Okanoue T, Fujiwara N, Okita K,

Kiyosawa K, Omata M, Kumada H, Hayashi N, Koike K. Clinical Characteristics, Treatment, and Prognosis of Non-B, Non-C Hepatocellular Carcinoma: A Large Retrospective Multicenter Cohort Study. J Gastroenterol 2014 [Epub].

3) Sato M, Kato N, Tateishi R, Muroyama R, Kowatari N, Li W, Goto K, Otsuka M, Shiina S, Yoshida H, Omata M, Koike K. Impact of Pnpla3 Polymorphisms on the Development of Hepatocellular Carcinoma in Patients with Chronic Hepatitis C Virus Infection. Hepatol Res 2014;44(10): E137-44.

4) Fujiwara N, Tateishi R, Nakagawa H, Nakagomi R, Kondo M, Minami T, Sato M, Uchino K, Enooku K, Kondo Y, Asaoka Y, Shiina S, Yoshida H, Koike K. Slight Elevation of High-Sensitivity C-Reactive Protein to Predict Recurrence and Survival in Patients with Early Stage Hepatitis C-Related Hepatocellular Carcinoma. Hepatol Res 2014 [EPub].

5) He G, Dhar D, Nakagawa H, Font-Burgada J, Ogata H, Jiang Y, Shalapour S, Seki E, Yost SE, Jepsen K, Frazer KA, Harismendy O, Hatziapostolou M, Iliopoulos D, Suetsugu A, Hoffman RM, Tateishi R, Koike K, Karin M. Identification of Liver Cancer Progenitors Whose Malignant Progression Depends on Autocrine Il-6 Signaling. Cell 2013;155(2): 384-96.

6) Masuzaki R, Tateishi R, Yoshida H, Arano T, Uchino K, Enooku K, Goto E, Nakagawa H, Asaoka Y, Kondo Y, Goto T, Ikeda H, Shiina S, Omata M, Koike K. Assessment of disease progression in patients with transfusion-associated chronic hepatitis C using transient elastography. World J Gastroenterol 2012;18(12): 1385-90.

2. 学会発表

1) 榎奥健一郎，建石良介，奥新和也，中込良，近藤真由子，藤原直人，南達也，佐藤雅哉，内野康志，浅岡良成，近藤祐嗣，藤永秀剛，堤武也，森屋恭爾，四柳宏，小池和彦．非 B 非 C 肝障害患者での CAP/Fibroscan 測定データの解析．第 22 回日本消化器関連学会週間，神戸，2014

2) 建石良介，岡上武，小池和彦．糖尿病治療内容が非 B 非 C 肝癌発癌年齢に与える影響．第 22 回日本消化器関連学会週間，神戸，2014

3) Fujiwara N, Tateishi R, Ryo Nakagomi, Mayuko Kondo, Minami T, Sato M, Uchino K, Enooku K, Nakagawa H, Kondo Y, Asaoka Y, Shiina S, and Koike K. Associations between body mass index, body composition and survival in patients with hepatocellular carcinoma. International Liver Cancer Association 8th Annual Conference. Kyoto, Japan, 2014

4) Tateishi R, Okanoue T, Fujiwara N, Okita K, Kiyosawa K, Omata M, Kumada H, Hayashi N, and Koike K for the INUYAMA NOBLESSE Study Group, Categorization of non-B, non-C hepatocellular carcinoma patients using hierarchical clustering, The annual meeting of American Association for

the Study of the Liver Diseases, Washington DC, USA, 2013
5) 建石良介、岡上武、小池和彦、非B非C肝細胞癌の現況と問題点、第49回日本肝癌研究会、東京、2013
6) 建石良介，榎奥健一郎，小池和彦．非B非C肝細胞癌の囲い込みは可能か? 第20回日本消化器関連学会週間、神戸、2012年

H. 知的所有権の出願・取得状況

1.特許取得

なし

2.実用新案登録

なし

3.その他

なし

研究成果の刊行に関する一覧表

雑誌

発表者氏名	論文タイトル名	発表誌名	巻号	ページ	出版年
Watanabe Y, Yamamoto H, Oikawa R, Toyota M, Yamamoto M, Kokudo N, Tanaka S, Arii S, Yotsuyanagi H, Koike K, Itoh F.	DNA methylation at hepatitis B viral integrants is associated with methylation at flanking human genomic sequences	Genome Res	25	328-337	2015
Sekine S, Ito K, Watanabe H, Nakano T, Moriya K, Shintani Y, Fujie H, Tsutsumi T, Miyoshi H, Fujinaga H, Shinzawa S, Koike K, Horie T	Mitochondrial iron accumulation exacerbates hepatic toxicity caused by hepatitis C virus core protein	Toxicol Appl Pharmacol	282	237-243	2015
Nakagawa H, Umemura A, Taniguchi K, Font-Burgada J, Dhar D, Ogata H, Zhong Z, Valasek MA, Seki E, Hidalgo J, Koike K, Kaufman RJ, Karin M.	ER Stress Cooperates with Hypernutrition to Trigger TNF-Dependent Spontaneous HCC Development	Cancer Cell	26	331-343	2014
Ohno M, Otsuka M, Kishikawa T, Shibata C, Yoshikawa T, Takata A, Muroyama R, Kowatari N, Sato M, Kato N, Kuroda S, Koike K	Specific delivery of microRNA93 into HBV-replicating hepatocytes downregulates protein expression of liver cancer susceptible gene MICA	Oncotarget	5(14)	5581-90	2014
Shibata C, Ohno M, Otsuka M, Kishikawa T, Goto K, Muroyama R, Kato N, Yoshikawa T, Takata A, Koike K	The flavonoid apigenin inhibits hepatitis C virus replication by decreasing mature microRNA122 levels	Virology	462-463	42-48	2014
Kondo M, Ishizawa T, Enooku K, Tokuhara Y, Ohkawa R, Uranbileg B, Nakagawa H, Tateishi R, Yoshida H, Kokudo N, Koike K, Yatomi Y, Ikeda H	Increased serum autotaxin levels in hepatocellular carcinoma patients were caused by background liver fibrosis but not by carcinoma	Clin Chim Acta	433	128-134	2014
Nguyen T, Xu J, Chikuma S, Hiai H, Kinoshita K, Moriya K, Koike K, Marcuzzi GP, Pfister H, Honjo T, Kobayashi M	Activation-induced cytidine deaminase is dispensable for virus-mediated liver and skin tumor development in mouse models	Int Immunol	26(7)	397-406	2014
Kumada H, Suzuki Y, Ikeda K, Toyota J, Karino Y, Chayama K, Kawakami Y, Ido A, Yamamoto K, Takaguchi K, Izumi N, Koike K, Takehara T, Kawada N, Sata M, Miyagoshi H, Eley T, McPhee F, Damokosh A, Ishikawa H, Hughes E	Daclatasvir plus asunaprevir for chronic HCV genotype 1b infection	Hepatology	59(6)	2083-2091	2014
Enooku K, Nakagawa H, Soroida Y, Ohkawa R, Kageyama Y, Uranbileg B, Watanabe N, Tateishi R, Yoshida H, Koike K, Yatomi Y, Ikeda H	Increased serum mitochondrial creatine kinase activity as a risk for hepatocarcinogenesis in chronic hepatitis C patients	Int J Cancer	135(4)	871-879	2014
Sato M, Kato N, Tateishi R, Muroyama R, Kowatari N, Li W, Goto K, Otsuka M, Shiina S, Yoshida H, Omata M, Koike K	IL28B minor allele is associated with a younger age of onset of hepatocellular carcinoma	J Gastroenterol	49(4)	748-754	2014

	in patients with chronic hepatitis C virus infection				
Sato M, Kondo M, Tateishi R, Fujiwara N, Kato N, Yoshida H, Taguri M, Koike K	Impact of IL28B Genetic Variation on HCV-Induced Liver Fibrosis, Inflammation, and Steatosis: A Meta-Analysis	PLoS One	9(3)	e91822	2014
Otsuka M, Kishikawa T, Yoshikawa T, Ohno M, Takata A, Shibata C, Koike K	The role of microRNAs in hepatocarcinogenesis: current knowledge and future prospects	J Gastroenterol	49(2)	173-184	2014
Yotsuyanagi H, Ito K, Yamada N, Takahashi H, Okuse C, Yasuda K, Suzuki M, Moriya K, Mizokami M, Miyakawa Y, Koike K	High levels of HBV after the onset lead to chronic infection in patients with acute hepatitis B	Clin Infect Dis	57(7)	935-942	2014
Shibata C, Kishikawa T, Otsuka M, Ohno M, Yoshikawa T, Takata A, Yoshida H, Koike K	Inhibition of microRNA122 decreases SREBP1 expression by modulating suppressor of cytokine signaling 3 expression	Biochem Biophys Res Commun	438(1)	230-235	2014
Yuhashi K, Ohnishi S, Kodama T, Koike K, Kanamori H	In vitro selection of the 3'-untranslated regions of the human liver mRNA that bind to the HCV nonstructural protein 5B	Virology	450-451	13-23	2014
Hikita H, Enooku K, Satoh Y, Yoshida H, Nakagawa H, Masuzaki R, Tateishi R, Soroida Y, Sato M, Suzuki A, Gotoh H, Iwai T, Yokota H, Koike K, Yatomi Y, Ikeda H.	Perihepatic lymph node enlargement is a negative predictor for sustained responses to pegylated interferon-α and ribavirin therapy for Japanese patients infected with hepatitis C virus genotype 1.	Hepatol Res	43(10)	1005-1012	2013
He G, Dhar D, Nakagawa H, Font-Burgada J, Ogata H, Jiang Y, Shalapour S, Seki E, Yost SE, Jepsen K, Frazer KA, Harismendy O, Hatziapostolou M, Iliopoulos D, Suetsugu A, Hoffman RM, Tateishi R, Koike K, Karin M	Identification of Liver Cancer Progenitors Whose Malignant Progression Depends on Autocrine IL-6 Signaling	Cell	155(2)	384-396	2013
Kishikawa T, Otsuka M, Yoshikawa T, Ohno M, Takata A, Shibata C, Kondo Y, Akanuma M, Yoshida H, Koike K.	Regulation of the expression of the liver cancer susceptibility gene MICA by microRNAs.	Sci Rep	3	2739	2013
Koike K.	The oncogenic role of hepatitis C virus.	Recent Results Cancer Res	193	97-111	2014
Ohno M, Shibata C, Kishikawa T, Yoshikawa T, Takata A, Kojima K, Akanuma M, Kang YJ, Yoshida H, Otsuka M, Koike K.	The flavonoid apigenin improves glucose tolerance through inhibition of microRNA maturation in miRNA103 transgenic mice.	Sci Rep	3	2553	2013
Urabe Y, Ochi H, Kato N, Kumar V, Takahashi A, Muroyama R, Hosono N, Otsuka M, Tateishi R, Lo PH, Tanikawa C, Omata M,	A genome-wide association study of HCV induced liver cirrhosis in the Japanese population	J Hepatol	58(5)	875-882	2013

Koike K, Miki D, Abe H, Kamatani N, Toyota J, Kumada H, Kubo M, Chayama K, Nakamura Y, Matsuda K.	identifies novel susceptibility loci at MHC region.				
Hikita H, Nakagawa H, Tateishi R, Masuzaki R, Enooku K, Yoshida H, Omata M, Soroida Y, Sato M, Gotoh H, Suzuki A, Iwai T, Yokota H, Koike K, Yatomi Y, Ikeda H.	Perihepatic lymph node enlargement is a negative predictor of liver cancer development in chronic hepatitis C patients.	J Gastroenterol	48(3)	366-373	2013
Lo PH, Urabe Y, Kumar V, Tanikawa C, Koike K, Kato N, Miki D, Chayama K, Kubo M, Nakamura Y, Matsuda K.	Identification of a functional variant in the mica promoter which regulates mica expression and increases HCV-related hepatocellular carcinoma risk.	PLoS One	8(4)	e61279	2013
Takata A, Otsuka M, Yoshikawa T, Kishikawa T, Hikiba Y, Obi S, Goto T, Kang YJ, Maeda S, Yoshida H, Omata M, Asahara H, Koike K.	MiRNA-140 acts as a liver tumor suppressor by controlling NF-κB activity via directly targeting Dnmt1 expression.	Hepatology	57	162-170	2013
Shiina S, Tateishi R, Imamura M, Teratani T, Koike Y, Sato S, Obi S, Kanai F, Kato N, Yoshida H, Omata M, Koike K	Percutaneous ethanol injection for hepatocellular carcinoma: 20-year outcome and prognostic factors	Liver Int	32(9)	1434-1442	2012
Kegeyama Y, Ikeda H, Watanabe N, Nagamine M, Kusumoto Y, Yashiro M, Satoh Y, Shimosawa T, Shinozaki K, Tomiya T, Inoue Y, Nishikawa T, Ohtomo N, Tanoue Y, Yokota H, Koyama T, Ishimaru K, Okamoto Y, Takuwa Y, Koike K, Yatomi Y.	Antagonism of sphingosine 1-phosphate receptor 2 causes a selective reduction of portal vein pressure in bile duct-ligated rats	Hepatology	56(4)	1427-1438	2012
Kumar V, Yi Lo PH, Sawai H, Kato N, Takahashi A, Deng Z, Urabe Y, Mbarek H, Tokunaga K, Tanaka Y, Sugiyama M, Mizokami M, Muroyama R, Tateishi R, Omata M, Koike K, Tanikawa C, Kamatani N, Kubo M, Nakamura Y, Matsuda K	Soluble MICA and a MICA Variation as Possible Prognostic Biomarkers for HBV-Induced Hepatocellular Carcinoma	PLoS One	7(9)	e44743	2012
Nakagawa H, Isogawa A, Tateishi R, Tani M, Yoshida H, Yamakado M, Koike K	Serum gamma-glutamyltransferase level is associated with serum superoxide dismutase activity and metabolic syndrome in a Japanese population	J Gastroenterol	47(2)	187-194	2012
Soroida Y, Ohkawa R, Nakagawa H, Satoh Y, Yoshida H, Kinoshita H, Tateishi R, Masuzaki R, Enooku K, Shiina S, Sato T, Obi S, Hoshino T, Nagatomo R, Okubo S, Yokota H, Koike K, Yatomi Y, Ikeda H	Increased activity of serum mitochondrial isoenzyme of creatine kinase in hepatocellular carcinoma patients predominantly with recurrence	J Hepatol	27(2)	330-336	2012
Shiina S, Tateishi R, Arano T, Uchino K, Enooku K, Nakagawa H, Asaoka Y, Sato T, Masuzaki R, Kondo Y, Goto T, Yoshida H, Omata M, Koike K	Radiofrequency ablation for hepatocellular carcinoma: 10-year outcome and prognostic factors	Am J Gastroenterol	107(4)	569-577	2012

Yasui K, Kawaguchi T, Shima T, Mitsuyoshi H, Seki K, Sendo R, Mizuno M, Itoh Y, Matsuda F, Okanoue T..	Effect of PNPLA3 rs738409 variant (I148M) on hepatic steatosis, necroinflammation, and fibrosis in Japanese patients with chronic hepatitis C	J Gastroenterol			2014 Nov 28. [Epub ahead of print]
Yamaguchi K, Nishimura T, Ishiba H, Seko Y, Okajima A, Fujii H, Tochiki N, Umemura A, Moriguchi M, Sumida Y, Mitsuyoshi H, Yasui K, Minami M, Okanoue T, Itoh Y.	Blockade of interleukin 6 signaling ameliorates systemic insulin resistance through upregulation of glucose uptake in skeletal muscle and improves hepatic steatosis in high –fat diet mice.	Liver Int			2014 Jul 26. Doi: 10. 1111/liv. 12645. [Epud ahead of print]
Kawaguchi T, Sumida Y, Umemura A, Matsuo K, Takahashi M, Takamura T, Yasui K, Saibara T, Hashimoto E, Kawanaka M, Watanabe S, Kawata S, Imai Y, Kokubo M, Shima T, Park H, Tanaka H, Tajima K, Yamada R, Matsuda F, Okanoue T, Japan Study Group of Nonalcoholic Fatty Liver Disease.	Genetic polymorphisms of the human PNPLA3 gene are strongly associated with severity of non-alcoholic fatty liver disease in Japanese	PLoS One	7	e38322	2012
Tokushige K, Hashimoto E, Horie Y, Taniai M, Higuchi S.	Hepatocellular carcinoma based on cryptogenic liver disease: The most common non-viral hepatocellular carcinoma in patients aged over 80 years.	Hepatol Res.	Jun 13	doi: 0.1111/ hepr.12372.	2014
Hashimoto E, Taniai M, Tokushige K.	Characteristics and diagnosis of NAFLD/NASH.	J Gastroenterol Hepatol	28 Suppl 4	64-70	2013
TokushigeK, HashimotoE, Kodama K.	Hepatocarcinogenesis in non-alcoholic fatty liver disease in Japan.	J Gastroenterol Hepatol	28 Suppl 4	88-92	2013
Kudo A, Tanaka S, Ban D, Matsumura S, Irie T, Ochiai T, Nakamura N, Arii S, Tanabe M.	Alcohol consumption and recurrence of non-B or non-C hepatocellular carcinoma after hepatectomy: a propensity score analysis.	Journal of Gastroenterology	49(9)	1352-1361.	2014
Muramatsu S, Tanaka S, Mogushi K, Adikrisna R, Aihara A, Ban D, Ochiai T, Irie T, Kudo A, Nakamura N, Tanaka H, Nakayama K, Tanaka H, Yamaoka S, Arii S.	Visualization of stem cell features in human hepatocellular carcinoma enlightened in vivo significance of tumor-host interaction and clinical implication.	Hepatology	58(1)	218-228	2013

Matsumura S, Imoto I, Kozaki K, Matsui T, Muramatsu T, Furuta M, Tanaka S, Sakamoto M, Arii S, Inazawa J.	Integrative array-based approach identifies MZB1 as a frequently methylated putative tumor-suppressor in hepatocellular carcinoma.	Clinical Cancer Research	18(13)	3541-3551	2012
Okada-Iwabu M, Yamauchi T, Iwabu M, Honma T, Hamagami K, Matsuda K, Yamaguchi M, Tanabe H, Kimura-Someya T, Shirouzu M, Ogata H, Tokuyama K, Ueki K, Nagano T, Tanaka A, Yokoyama S, Kadowaki T.	A small-molecule AdipoR agonist for type 2 diabetes and short life in obesity.	Nature	503	493-499	2013
Nio Y, Yamauchi T, Iwabu M, Okada-Iwabu M, Funata M, Yamaguchi M, Ueki K, Kadowaki T	Monocyte chemoattractant protein-1 (MCP-1) deficiency enhances alternatively activated M2 macrophages and ameliorates insulin resistance and fatty liver in lipoatrophic diabetic A-ZIP transgenic mice.	Diabetologia	55	3350-3358	2012
Seko Y, Akuta N, Suzuki F, Kawamura Y,Sezaki H, Sezaki H, Suzuki Y, Hosaka T, Kobayashi M, Kobayashi M, Saitoh S, Arase Y, Ikeda K. Kumada H	Amino acid substitutions in the hepatitis C virus core region and lipid metabolosm are associated with hepatocarcinogenesis in nonresponders to interferon plus ribavirin combination therapy.	Intervirology.	56	13-21	2013
Arase Y, Kobayashi M, Suzuki F, Suzuki Y, Kawamura Y, Akuta N, Kobayashi M, Sezaki H, Saito S, Hosaka T, Ikeda K, Kumada H, Kobayashi T.	Effect of type 2 diabetes on risk for malignancies included hepatocellular carcinoma in chronic hepatitis C.	Hepatology.	57	964-973	2013
Akuta N, Suzuki F, Seko Y, Kawamura Y, Sezaki H, Suzuki Y, Hosaka T, Kobayashi M, Hara T, Kobayashi M, Saitoh S, Arase Y, Ikeda K, Kumada H.	Complicated relationships of amino acid substitution in hepatitis C virus core region and *IL28B* genotype influencing hepatocarcinogenesis.	Hepatology.	56	2134-2141	2012
Kawaguchi T, Itou M, Taniguchi E, Sata M	Exendin-4, a glucagon-like peptide-1 receptor agonist, modulates hepatic fatty acid composition and Δ-5-desaturase index in a murine model of non-alcoholic steatohepatitis	Int J Mol Med.	34(3)	782-787	2014
Kawaguchi T, Nagao Y, Sata M	Independent factors associated with altered plasma active ghrelin levels in HCV-infected patients	Liver Int.	33(10)	1510-1516	2013

Taniguchi E, Kawaguchi T, Sakata M, Itou M, Oriishi T, Sata M	Lipid profile is associated with the incidence of cognitive dysfunction in viral cirrhotic patients: A data-mining analysis	Hepatol Res.	43(4)	418-424	2013
Otsuka M, Uchida Y, Kawaguchi T, Taniguchi E, Kawaguchi A, Kitani S, Itou M, Oriishi T, Kakuma T, Tanaka S, Yagi M, Sata M.	Fish to meat intake ratio and cooking oils are associated with hepatitis C virus carriers with persistently normal alanine aminotransferase levels.	Hepatol Res	42(10)	982-989	2012
Fukuhara T, Wada M, Nakamura S, Ono C, Shiokawa M, Yamamoto S, Motomura T, Okamoto T, Okuzaki D, Yamamoto M, Saito I, Wakita T, Koike K, and Matsuura Y.	Amphipathic α-Helices in apolipoproteins are crucial to the formation of infectious hepatitis C virus particles.	PLoS Pathog		doi: 10.1371/journal.ppat.1004534	2014
Shiokawa M, Fukuhara T, Ono C, Yamamoto S, Okamoto T, Watanabe N, Wakita T, and Matsuura Y.	Novel permissive cell lines for a complete propagation of hepatitis C virus.	J Virol	88	5578-5594	2014
Fukuhara T, Kambara H, Shiokawa M, Ono C, Katoh H, Morita E, Okuzaki D, Maehara Y, Koike K, and Matsuura Y.	Expression of miR-122 facilitates an efficient replication in nonhepatic cells upon infection with HCV.	J Virol	86	7918-7933	2012
Kambara H, Fukuhara T, Shiokawa M, Ono C, Ohara Y, Kamitani W, and Matsuura Y.	Establishment of a novel permissive cell line for propagation of hepatitis C virus by the expression of microRNA122.	J Virol	86	1382-1393	2012
Mawatari S., Uto H., Ido A., Nakashima K., Suzuki T., Kanmura S., Kumagai K., Oda K., Tabu K., Tamai T., Moriuchi A., Oketani M., Shimada Y., Sudoh M., Shoji I., and Tsubouchi H.	Hepatitis C virus NS3/4A protease inhibits complement activation by cleaving complement component 4.	PLoS One	8	e82094, 1-7	2013
El-Shamy A, Shindo M, Shoji I, Deng L, Okuno T, and Hotta H.	Polymorphisms of the Core, NS3 and NS5A proteins of hepatitis C virus genotype 1b associate with development of hepatocellular carcinoma.	Hepatology	58	555-563	2013
Matsui, C., Shoji, I., Kaneda, S., Sianipar, IR., Deng, L., and Hotta, H.	Hepatitits C virus infection suppresses GLUT2 gene expression via down-regulation of hepatocyte nuclear factor 1α.	Journal of Virology	86	12903-11	2012
Sekine S, Ito K, Watanabe H, Nakano T, Moriya K, Shintani Y, Fujie H, Tsutsumi T, Miyoshi H, Fujinaga H, Shinzawa S, Koike K, Horie T.	Mitochondrial iron accumulation exacerbates hepatic toxicity caused by hepatitis C virus core protein.	Toxicol Appl Pharmacol.	Dec 27;282(3):237-243	237-243	2014

Horiuchi Y, Takagi A, Kobayashi N, Moriya O, Nagai T, Moriya K, Tsutsumi T, Koike K, Akatsuka T.	Effect of the infectious dose and the presence of hepatitis C virus core gene on mouse intrahepatic CD8 T cells.	Hepatol Res.	44 (10)	240-252	2014
Tateishi R, Okanoue T, Fujiwara N, Okita K, Kiyosawa K, Omata M, Kumada H, Hayashi N, Koike K.	Clinical Characteristics, Treatment, and Prognosis of Non-B, Non-C Hepatocellular Carcinoma: A Large Retrospective Multicenter Cohort Study.	J Gastroenterol	[Epub]		2014
He G, Dhar D, Nakagawa H, Font-Burgada J, Ogata H, Jiang Y, Shalapour S, Seki E, Yost SE, Jepsen K, Frazer KA, Harismendy O, Hatziapostolou M, Iliopoulos D, Suetsugu A, Hoffman RM, Tateishi R, Koike K, Karin M.	Identification of Liver Cancer Progenitors Whose Malignant Progression Depends on Autocrine Il-6 Signaling	Cell	155(2)	284-96	2013

DNA methylation at hepatitis B viral integrants is associated with methylation at flanking human genomic sequences

Yoshiyuki Watanabe,[1,2,9] Hiroyuki Yamamoto,[1,9] Ritsuko Oikawa,[1] Minoru Toyota,[3] Masakazu Yamamoto,[4] Norihiro Kokudo,[5] Shinji Tanaka,[6] Shigeki Arii,[6] Hiroshi Yotsuyanagi,[7] Kazuhiko Koike,[8] and Fumio Itoh[1]

[1]*Division of Gastroenterology and Hepatology, Department of Internal Medicine, St. Marianna University School of Medicine, Kawasaki 216-8511, Japan;* [2]*Internal Medicine, Kawasaki Rinko General Hospital, Kawasaki 210-0806, Japan;* [3]*Department of Molecular Biology, Sapporo Medical University School of Medicine, Sapporo 060-8556, Japan;* [4]*Department of Surgery, Institute of Gastroenterology, Tokyo Women's Medical University, Tokyo 162-8666, Japan;* [5]*Hepato-Biliary-Pancreatic Surgery Division, Artificial Organ and Transplantation Division, Department of Surgery, Graduate School of Medicine, University of Tokyo 113-8655, Japan;* [6]*Department of Hepatobiliary Pancreatic Surgery, Graduate School, Tokyo Medical and Dental University, Tokyo 113-0034, Japan;* [7]*Department of Infectious Diseases, Graduate School of Medicine, University of Tokyo, Tokyo 113-8655, Japan;* [8]*Department of Gastroenterology, Graduate School of Medicine, University of Tokyo, Tokyo 113-8655, Japan*

Integration of DNA viruses into the human genome plays an important role in various types of tumors, including hepatitis B virus (HBV)–related hepatocellular carcinoma. However, the molecular details and clinical impact of HBV integration on either human or HBV epigenomes are unknown. Here, we show that methylation of the integrated HBV DNA is related to the methylation status of the flanking human genome. We developed a next-generation sequencing-based method for structural methylation analysis of integrated viral genomes (denoted G-NaVI). This method is a novel approach that enables enrichment of viral fragments for sequencing using unique baits based on the sequence of the HBV genome. We detected integrated HBV sequences in the genome of the PLC/PRF/5 cell line and found variable levels of methylation within the integrated HBV genomes. Allele-specific methylation analysis revealed that the HBV genome often became significantly methylated when integrated into highly methylated host sites. After integration into unmethylated human genome regions such as promoters, however, the HBV DNA remains unmethylated and may eventually play an important role in tumorigenesis. The observed dynamic changes in DNA methylation of the host and viral genomes may functionally affect the biological behavior of HBV. These findings may impact public health given that millions of people worldwide are carriers of HBV. We also believe our assay will be a powerful tool to increase our understanding of the various types of DNA virus-associated tumorigenesis.

[Supplemental material is available for this article.]

Hepatitis B virus (HBV) infects more than two billion people worldwide, and 400 million chronically infected individuals are at high risk of developing active hepatitis, cirrhosis, and hepatocellular carcinoma (HCC) (Gatza et al. 2005; Lupberger and Hildt 2007). HBV carriers with chronic liver disease are at a 100-fold greater risk of developing HCC, which is the third leading cause of cancer-related death worldwide. The HBV genome is integrated into the host genome in 90% of patients with HCC (HBV-HCC) (Gatza et al. 2005; Lupberger and Hildt 2007). HBV-HCCs have been analyzed by comprehensive genome sequencing and high-resolution genome mapping (Kan et al. 2013; Li and Mao 2013; Nakagawa and Shibata 2013). Moreover, the recent deep sequencing of HBV DNA in patients with HCC revealed increased integration events, structural alterations, and sequence variations (Ding et al. 2012; Fujimoto et al. 2012; Jiang et al. 2012; Sung et al. 2012; Toh et al. 2013). A recent study identified a viral-human chimeric fusion transcript, HBx-LINE1, that functions like a long noncoding RNA to promote HCC (Lau et al. 2014). However, the molecular details and clinical impact of HBV integration on the epigenomes of human cells and HBV remain to be defined.

Methylation of exogenous DNA (including viral DNA) that is integrated into the human genome has been studied over the past decade (Doerfler et al. 2001). Within the human genome, cytosine methylation in CpG dinucleotides (CpG sites), which cluster into islands associated with transcriptional promoters, is an important mechanism for regulating gene expression. Additionally, host cells use methylation as a defense mechanism against foreign agents (e.g., viral DNA) (Doerfler 2008; Doerfler et al. 2001). DNA methylation suppresses the expression of viral genes and other deleterious elements incorporated into the host genome over time. Establishment of de novo patterns of DNA methylation is char-

[9]**These authors contributed equally to this work.**
Corresponding author: h-yama@marianna-u.ac.jp.
Article published online before print. Article, supplemental material, and publication date are at http://www.genome.org/cgi/doi/10.1101/gr.175240.114.

25:328–337 Published by Cold Spring Harbor Laboratory Press; ISSN 1088-9051/15; www.genome.org

acterized by the gradual spread of methylation (Orend et al. 1991). Another attractive possibility is that DNA methylation camouflages the virus from the immune system (Tao and Robertson 2003; Hilleman 2004), resulting in a DNA methylation–related blockade of viral antigen presentation that allows the virus to escape immune control (Fernandez et al. 2009).

The DNA methylome of HBV in human cells may undergo dynamic changes at different stages of disease (Fernandez et al. 2009). For example, DNA methylation at the *HBVgp2* locus, which codes for the S viral proteins, reportedly increases during the progression from asymptomatic lesions to benign lesions, to premalignant disease and malignant tumors. However, because of the significant deletions of the integrated HBV genome detected in this previous study (Fernandez et al. 2009), the DNA methylome of HBV needs to be further characterized. Moreover, the molecular mechanisms involved and the clinical impact of the integration of HBV on the human and HBV epigenomes are unknown. To address these issues, we developed a next-generation sequencing (NGS)–based method for methylation analysis of integrated viral genomes (denoted G-NaVI) and applied this method to the integrative genomic and epigenomic analysis of human hepatoma cell lines and tissues with integrated HBV genomes.

Results

DNA methylation levels in PLC/PRF/5 cells and cancerous tissues obtained from HBV-HCC patients

Methylated CpG island (CGI) amplification (MCA) coupled with microarray (MCAM) analysis (Toyota et al. 1999; Oishi et al. 2012) was performed to detect methylated genes in the human PLC/PRF/5 cell line and in six paired specimens of primary HBV-HCC and adjacent tissues. Compared with the DNA methylation of CGIs in the healthy peripheral blood leukocytes of volunteers or the noncancerous tissues, levels of DNA methylation were not remarkable in the PLC/PRF/5 cells and the cancerous tissues obtained from HBV-HCC patients (Supplemental Fig. 1). These results were confirmed by bisulfite pyrosequencing of candidate tumor-related genes.

DNA methylation of CGIs of *HBx*

We then focused on epigenetic changes in the viral genome. Based on the hidden Markov models for sequence analysis performed on the CpG plugin of bioinformatics software Geneious 5.5.8 (see Methods section), a CpG island was found in only the promoter region of the *HBx* gene in the HBV genome (Fig. 1A; Supplemental Fig. 2; Durbin et al. 1998; Kearse et al. 2012). Host signal transduction pathways and gene expression are disrupted by the expression of *trans*-activating factors derived from the HBV genome, such as the HBx protein and PreS2 activators (Gatza et al. 2005; Lupberger and Hildt 2007). Moreover, transgenic mice expressing high levels of HBx in the liver develop HCC (Kim et al.1991; Koike et al. 1994). The DNA methylation levels of the CGIs of *HBx* were analyzed in 10 HBV-HCC samples and 10 adjacent samples, as well as samples of PLC/PRF/5 cells by bisulfite pyrosequencing (Fig. 1A; Supplemental Fig. 2). We performed advanced methylation quantification in long sequence runs by pyrosequencing on PyroMark Q24 Advanced and PyroMark Q24 instruments. Methylation levels of *HBx* varied across samples (Fig. 1B,C) and were generally lower in HCC tissues than in the adjacent tissues (Fig. 1B). This finding is consistent with a previous report that most HBV genomes, although globally methylated to a greater extent in malignant samples than in premalignant lesions, retain *HBx* in an unmethylated state (Fernandez et al. 2009). Because the pyrosequencing results represent the genome-wide average of DNA methylation levels at the particular CpG site, the results could be affected by the HBV integration site. Therefore, genome-wide methylation analysis of the integrated HBV sequence is necessary in relation to the methylation state of the adjacent human genome. We did not detect an association between *HBx* methylation levels and those of the LINE1 and *Alu*Yb8 repeats (Fig. 1B).

Fluorescence in situ hybridization (FISH) and *Alu* PCR analyses of HBV integration

We developed a FISH technique for detecting HBV DNA in the genome of PLC/PRF/5 cells (Supplemental Figs. 3, 4). Twelve specific primer pairs (FISH probes 1–12) were designed based on the HBV sequences integrated into the genome of PLC/PRF/5 cells; amplification from all primer pairs was confirmed (Supplemental Fig. 4A). These results suggest full-length or partial HBV sequences that are covered by the 12 primer pairs were integrated into the genome of the PLC/PRF/5 cells. The FISH probes were labeled with digoxigenin, and FISH was performed using Carnoy-fixed chromosomal and nuclear specimens. Multiple HBV fluorescent signals (green) were detected in the nuclei (Supplemental Fig. 4B) using probes for *HBx* and its CGI sequences (probes 5 and 6), but not with probes 1–4 or 7–12 (Supplemental Fig. 4C–E). *Alu*-PCR identified one *HBx* integration site in PLC/PRF/5 (Supplemental Fig. 5). The integrated *HBx* sequence was 213 bp and included a promoter region. The *HBx* gene body was located only 13 bases (ATG GCT GCT AGG T) from the transcription start site and was integrated into a noncoding region of the host genome. There were 200 bases of viral DNA sequence upstream of the *HBx* transcription start site. According to the human genome reference sequence (GRCh38) published by the Genome Reference Consortium, this integration site was identified as a noncoding region of host Chromosome 5 1,350,106–1,350,478 that is near the telomerase reverse transcriptase (*TERT*) gene (Supplemental Fig. 5).

NGS analysis of HBV DNA integration site sequences

We developed an NGS analysis technique for sequencing the HBV DNA integration sites (Supplemental Fig. 6A). For efficient genome analysis, we synthesized 12,391 custom baits based on the sequences of the HBV genotypes A to J and on those sequences present in the HBV-transformed PLC/PRF/5 cells that were not related to the human genome sequence (Supplemental Fig. 6B). The average read length was 333.14 bp with a modal length of ~500 bp (Supplemental Fig. 6C). The average read quality was 31.91, corresponding to >99.9% accuracy. We did not detect a common HBV integration site (Fig. 2). The integration sites in the PLC/PRF/5 genome included intergenic (39%), intronic (39%), promoter (8%), and divergent promoter (15%) regions but not exonic (0%) sequences (Fig. 2). HepG2.2.15 cells, which stably express and replicate HBV in a culture system, are derived from the human hepatoblastoma cell line HepG2 (Sells et al. 1987). In the HepG2.2.15 genome, the integration sites included intergenic (29%), intronic (57%), and other (14%) regions but not promoter (0%), divergent promoter (0%), or exonic (0%) sequences (Fig. 2).

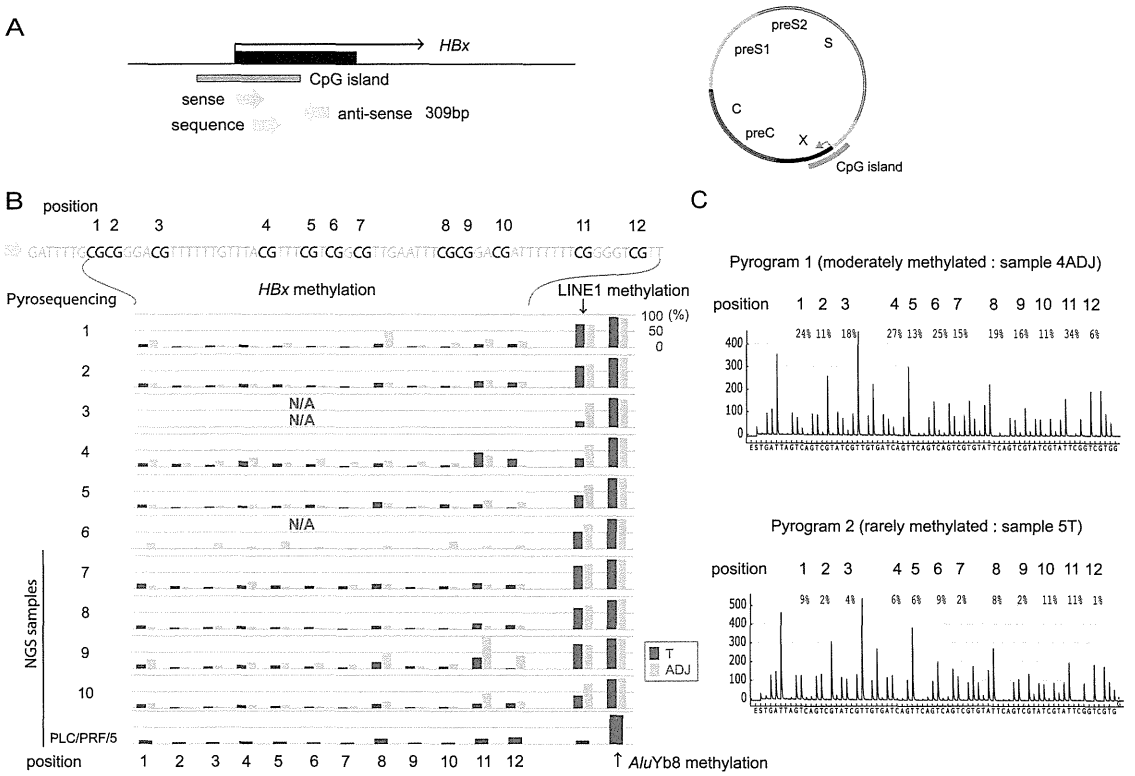

Figure 1. Methylation analysis of the CGI of the *HBx* gene. (*A*) Schema of the CGI of the *HBx* gene. Three arrows show the pyrosequencing primers used for the methylation analysis. (*B*) DNA methylation levels of the CpGs of the *HBx* gene, LINE1, and *AluYb8* in 10 paired HBV-HCC and adjacent nontumor tissue samples and PLC/PRF/5 DNA were analyzed using bisulfite pyrosequencing. Methylation levels of *HBx* varied across samples and were generally lower in HCC tissues than in the adjacent nontumor tissues. An association between *HBx* methylation levels and those of the LINE1 and *AluYb8* repeats was not observed. N/A, could not be analyzed. DNAs from four paired HBV-HCC and adjacent nontumor tissue samples (sample nos. 7–10), PLC/PRF5, and HepG2.2.15 were further analyzed using the NGS (G-NaVI method). (*C*) Representative pyrograms showing DNA methylation levels of the CpGs of the *HBx* gene. Methylation levels at 12 CpG sites of the *HBx* gene in adjacent nontumor tissue (sample no. 4ADJ) and tumor tissue (sample no. 5T) are shown.

DNA methylation of the integrated HBV genome as well as the adjacent human genome in cell lines

DNA methylation of the integrated HBV genome, as well as the adjacent human genome, was analyzed by bisulfite pyrosequencing. We detected varying levels of methylation of the HBV sequences integrated into the genome of PLC/PRF/5 cells (Fig. 3; Supplemental Fig. 7). Our data suggest DNA methylation in the integrated HBV genome is related to the methylation status of the integration sites within the human genome. We further characterized the methylation status of the HBV genome and human genome by allele-specific DNA methylation analysis (Fig. 3A), which revealed that the HBV genome often showed significant methylation when integrated into highly methylated sites in the human genome; however, the HBV genome remained largely unmethylated when integrated into unmethylated regions such as promoters (Fig. 3B). Integration of the HBV genome did not affect the methylation status of the human genome, including the promoter regions of the *TERT* and *SNX15* genes. Methylation of HBV DNA integrated into HepG2.2.15 cells transformed with HBV DNA (using a head-to-tail dimer) was further analyzed by bisulfite pyrosequencing, which revealed that the HBV genome generally showed significant methylation when integrated into highly methylated regions of the human genome; however, the HBV genome remains largely unmethylated when integrated into unmethylated regions (Fig. 3A).

DNA methylation levels in orthologous loci

We examined methylation levels of orthologous loci in HepG2.2.15 cells and in peripheral blood lymphocytes (PBLs) of a healthy volunteer and compared them to the methylation levels at the same (empty) target sites of PLC/PRF/5 cells. Methylation levels of orthologous loci in HepG2.2.15 cells and PBLs were generally similar to those of PLC/PRF/5 cells (Fig. 3B). Similarly, we examined methylation levels of orthologous loci in PLC/PRF/5 cells and in PBLs of a healthy volunteer and compared them to the methylation levels at the same (empty) target sites of HepG2.2.15 cells. Methylation levels of orthologous loci in PLC/PRF/5 cells and PBLs were also generally similar to those of HepG2.2.15 cells (Fig. 3B).

DNA methylation of the integrated HBV genome and the adjacent human genome in HCC tissues

To determine whether our results are relevant to human tumors, we used bisulfite pyrosequencing to investigate the methylation status of the HBV and human genomes in surgical specimen pairs of HCC and adjacent nontumor tissues. We detected no common HBV integration site (Fig. 4; Supplemental Fig. 8). Recurrent HBV integration into the *SLC6A13* gene was observed in cancerous tissues. Integration sites were rarely detected in exonic regions of the DNA from HBV-HCC samples (Fig. 4; Supplemental Fig. 8). Similar to the results obtained from the PLC/PRF/5 and HepG2.2.15 cells, our analysis revealed that the HBV genome became significantly

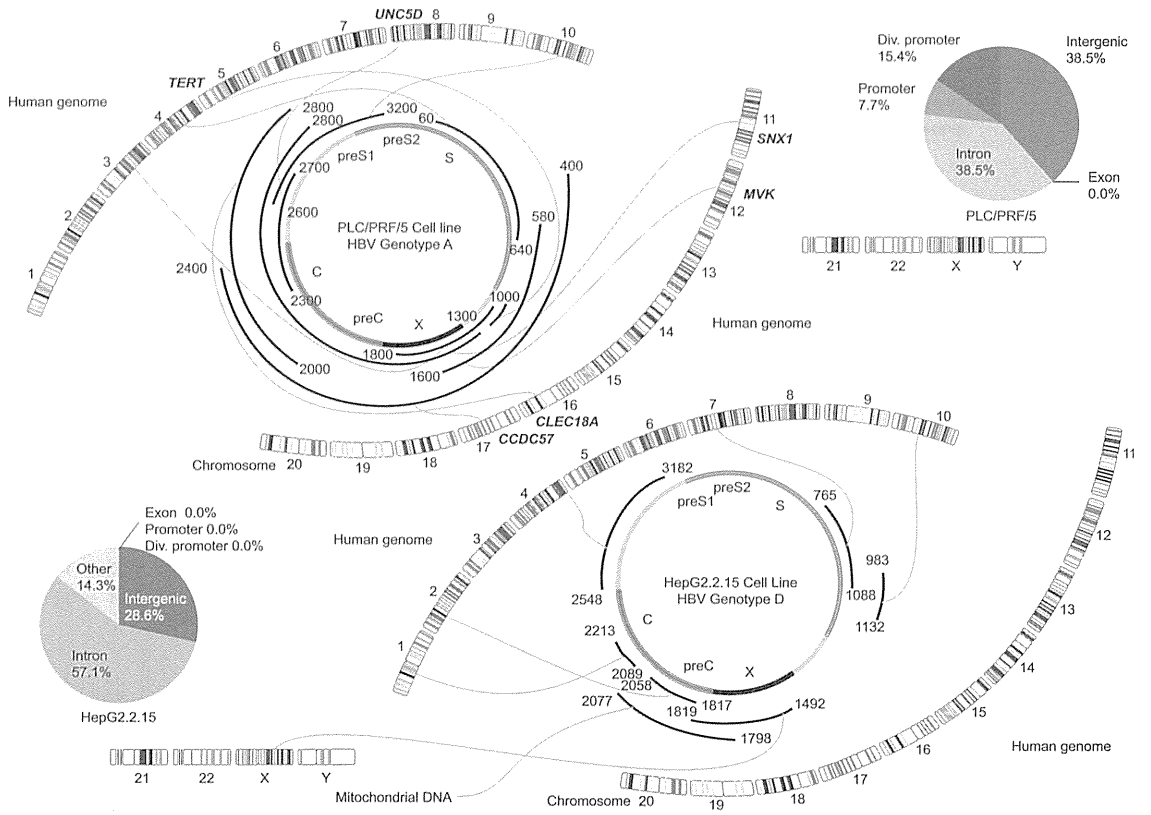

Figure 2. Distribution of the integration sites in the HBV genome and human chromosomes represented by Circos plots of the PLC/PRF/5 genome and the HepG2.2.15 genome. HBV DNA integration was analyzed using the G-NaVI method in the genome of PLC/PRF/5 cells and HepG2.2.15 cells. A common HBV integration site was not detected. Integration sites were not detected in exonic regions of the DNA from cell lines (Venn diagrams). The HBV genes (*PreC, Precore; C, Core; PreS, Presurface; S, Surface; X, X*) and the 24 human chromosomes are shown.

methylated when integrated into highly methylated human genome regions but not when integrated into unmethylated human genome regions (Fig. 4).

Correlation between the methylation pattern of the integrated HBV DNA and the human genome

DNA fragments, including 200 bp of the HBV DNA and 200 bp of the human genome around the boundary, were analyzed for average methylation, GC content, and repetitive sequences. A statistically significant correlation was observed between the average methylation of the HBV DNA and that of the human genome in cell lines and clinical samples (Fig. 5A–C; Supplemental Table 2). In contrast, average methylation did not correlate with GC content or repetitive sequences in the human and viral genome (Fig. 5D,E; Supplemental Table 2).

Using Bander software, we analyzed the chromatin structure at the integrated HBV site in PLC/PRF/5 and HepG2.2.15. Open chromatin and heterochromatin were observed more frequently at the integrated HBV in PLC/PRF/5 and HepG2.2.15, respectively (Supplemental Table 3). The difference may reflect the fact that PLC/PRF/5 is a naturally derived HBV-positive cell line and HepG2.2.15 is an HBV DNA-transfected cell line.

Discussion

We developed an NGS-based method for structural methylation analysis of integrated viral genomes. This method is a novel approach that enables the enrichment of viral fragments for sequencing using unique baits based only on the sequence of the HBV genome. We detected all regions of the human genome that harbored integrated HBV genomes without conducting unnecessary sequencing of regions where the HBV genome was not integrated. Because this technique only requires sequencing a small region of DNA around the integrated HBV sequences, a sufficient number of sequence reads can be acquired.

Methylation of viral DNA in infected cells may alter the expression patterns of viral genes related to infection and transformation (Burgers et al. 2007; Fernandez et al. 2009) and may clarify why certain infections are either cleared or persist with or without progression to precancer (Mirabello et al. 2012). To the best of our knowledge, we have, for the first time, established that the de novo patterns of DNA methylation in the integrated HBV genome are related to the methylation status of the integration sites within the human genome. A statistically significant correlation between the average methylation of the HBV DNA and that of the human genome in cell lines and clinical samples has greatly substantiated our findings. It is possible that the HBV genome becomes inactivated by methylation, when it is integrated into highly methylated host sites; therefore, HBV methylation may not contribute to tumor development. However, after integration into unmethylated human genome regions such as promoters, the HBV DNA remains unmethylated and may eventually play an important role in tumorigenesis (Fig. 6). Because multiple HBV integration sites were present in each of the analyzed samples, there remains the possibility of an asso-

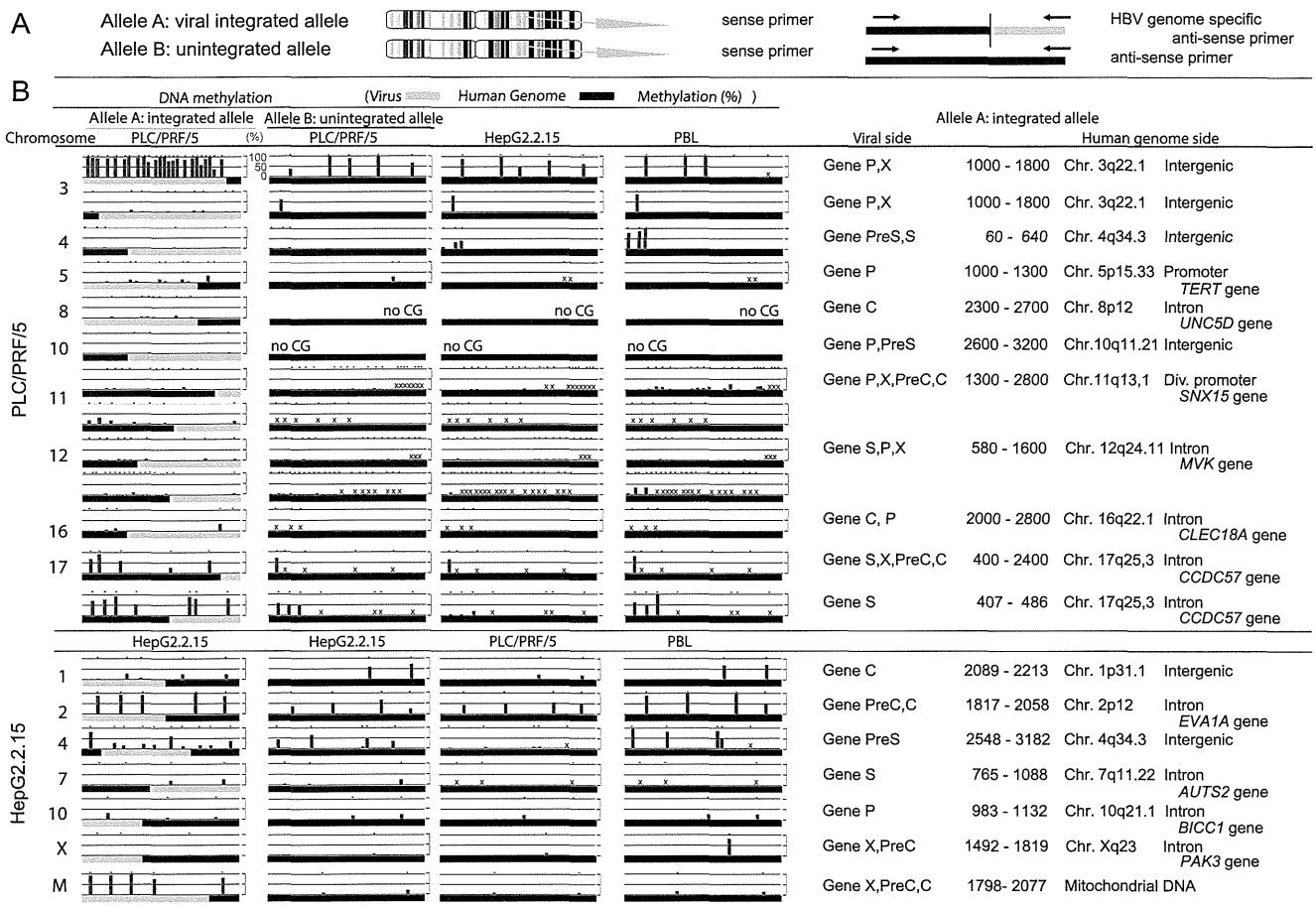

Figure 3. Allele-specific methylation analysis of the PLC/PRF/5 genome and the HepG2.2.15 genome. (*A*) A schema of allele-specific methylation analysis. (*B*) The methylation levels of the HBV and human genomes for the integrated and unintegrated alleles. Detailed results of the HBV integrants (*PreC, Precore; C, Core; PreS, Presurface; S, Surface; X, X*) and flanking host genomes (position, chromosome, location of the genome, and gene names) are shown. DNA methylation of the integrated HBV genome as well as the flanking human genome was examined by allele-specific DNA methylation analysis using bisulfite pyrosequencing. The HBV genome often showed significant methylation when integrated into highly methylated sites in the human genome; however, the HBV genome remained largely unmethylated when integrated into unmethylated regions. Methylation levels of orthologous loci in HepG2.2.15 cells and in PBLs of a healthy volunteer were examined and compared to the methylation levels at the same (empty) target sites of PLC/PRF/5 cells. Methylation levels of orthologous loci in HepG2.2.15 cells and PBLs were generally similar to those of PLC/PRF/5 cells. Similarly, methylation levels of orthologous loci in PLC/PRF/5 cells and in PBLs of a healthy volunteer were examined and compared to the methylation levels at the same (empty) target sites of HepG2.2.15 cells. Methylation levels of orthologous loci in PLC/PRF/5 cells and PBLs were generally similar to those of HepG2.2.15 cells. (×) The desired quantitative methylation levels were not obtained because of technical difficulties with the sequences that were being analyzed.

ciation between methylation and viral transcript levels. The biological impact of methylation on viral transcript levels or viral function, induced by viral insertions, also needs to be further addressed.

Methylation levels of orthologous loci in other samples at the same (empty) target sites of PLC/PRF/5 were generally similar to those of PLC/PRF/5. Similar results were observed in HepG2.2.15. These data suggest that a "before and after" relationship exists between methylation levels at preexisting target sites and those within viral insertions. At the same time, we cannot rule out the possibility that the integration of the virus subsequently affects the methylation established at the flanking target site, perhaps by acting in trans on the empty target site-containing allele. Therefore, this issue needs to be further addressed.

Differences in the integrated viral sequences could have a direct impact on the amount of cytosine methylation observed. In cases where the integration site is a highly active promoter, comparisons of methylation statuses may not be informative. Additional studies, using a large number of samples, are needed to address this issue.

Our results are notable because other studies have detected a statistically significant enrichment of HBV integration into regulatory regions, particularly promoters, in tumors (Sung et al. 2012; Toh et al. 2013); this observation may be explained by the relatively open chromatin structure of promoter regions. Average methylation did not correlate with GC content or repetitive sequences in the human and viral genomes. The relationship between methylation of HBV sequences and chromatin structure remains to be clarified because of the limitation of the Bander software used in this study. Although the mechanism needs clarification, the significant enrichment of HBV integration into regulatory regions would favor integrated HBV nonmethylation and lead to tumorigenesis. Alternatively, while the integration of HBV into the host genome may be random, HBV integration into regulatory regions is positively selected during tumorigenesis (Toh et al. 2013).

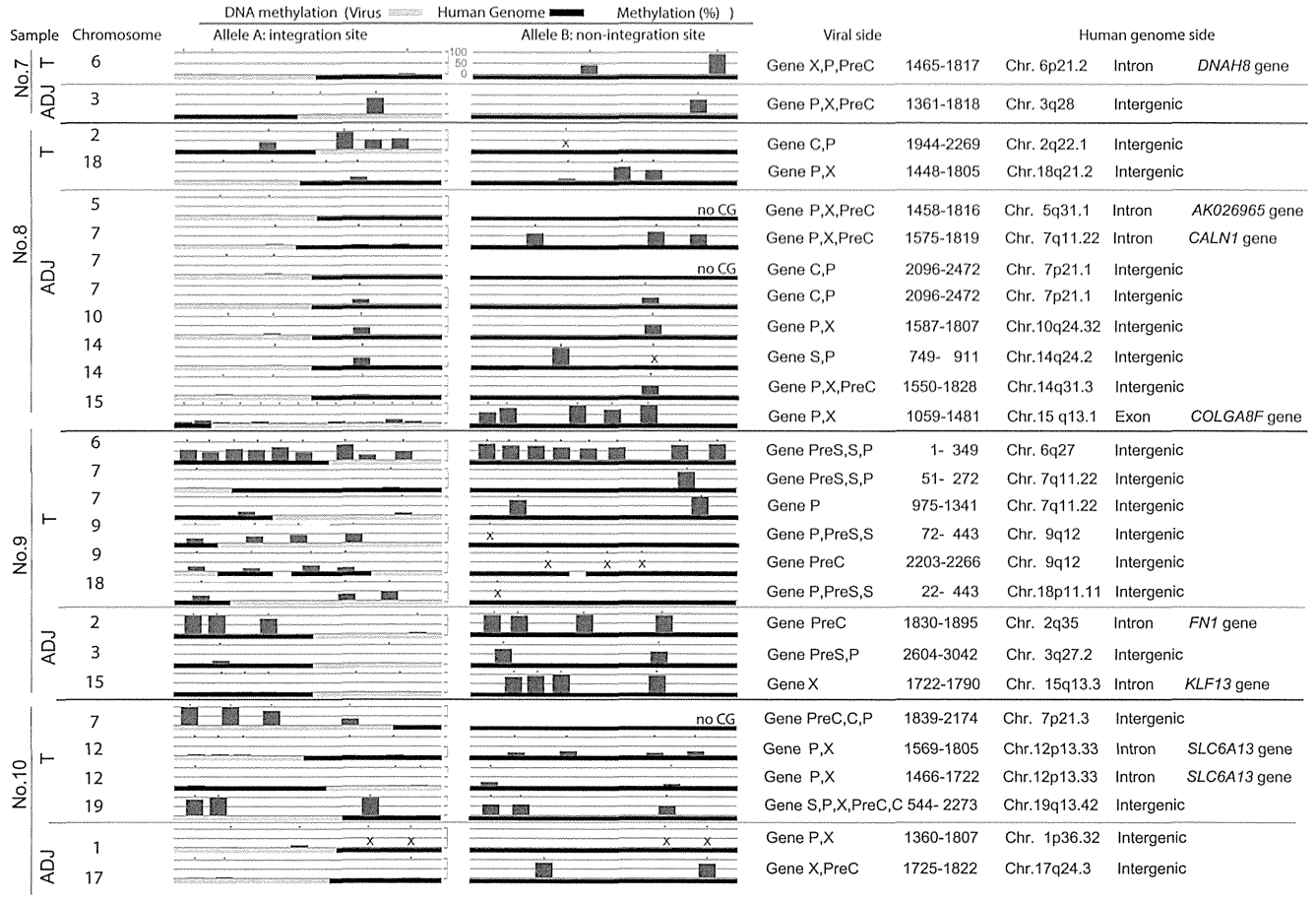

Figure 4. Allele-specific methylation analysis of the tumor (*T*) and adjacent nontumor (ADJ) sample genomes. The methylation levels of the HBV and human genomes for the integrated and unintegrated alleles in four paired tumor and adjacent nontumor samples (sample nos. 7–10) are shown. Detailed results of the HBV integrants (*PreC, Precore; C, Core; PreS, Presurface; S, Surface; X, X*) and flanking host genomes (position, chromosome, location of the genome, and gene names) are shown. The HBV genome became significantly methylated when integrated into highly methylated human genome regions, but not when integrated into unmethylated human genome regions. (×) The desired quantitative methylation levels were not obtained because of technical difficulties with the sequences that were being analyzed.

The dynamic changes in DNA methylation described here have a major functional impact on the biological behavior of HBV and underlie the molecular mechanisms that control infection or enable tumorigenesis. These findings may significantly impact public health given that millions of people worldwide are carriers of HBV. Distinct DNA methylation profiles may exist, for example, between primary HCCs in Japanese patients and those of other nationalities. Additional studies are needed to address this issue, and research into the influence of other environmental factors is required.

Increased viral DNA methylation is present in cancers associated with DNA viruses, including human papilloma virus types 16 and 18 (HPV 16 and 18) (Fernandez et al. 2009; Mirabello et al. 2012), Epstein-Barr virus (Uozaki and Fukayama 2008; Fernandez et al. 2009), and human T-lymphotropic virus 1 (Taniguchi et al. 2005). An analysis of the haplotype-resolved genome and epigenome of the aneuploid HeLa cervical cancer cell line revealed that an amplified, highly rearranged region of chromosome 8q24.21 harboring an integrated HPV18 genome likely represents the tumor-initiating event (Adey et al. 2013). Whether the dynamic changes in DNA methylation observed in cells with integrated HBV genomes also occur in human cells infected by other viruses is an interesting question for further study. We anticipate that our assay will be a powerful tool for this purpose and have successfully detected integrated HPV sequences in the genomes of cervical cancer cell lines (Y Watanabe, H Yamamoto, F Itoh, and N Suzuki, unpubl.).

This study provides novel mechanistic insights into HBV-mediated hepatocarcinogenesis, which may have preventive and therapeutic applications for carriers of HBV and patients with HBV-HCC, as it suggests that epigenetic alterations provide candidate biochemical markers and therapeutic targets. This study, together with a recent global survey of HBV integration events (Ding et al. 2012; Fujimoto et al. 2012; Jiang et al. 2012; Sung et al. 2012; Toh et al. 2013), provides a foundation for the further experimentation and mechanistic understanding of HBV-HCC.

Methods

Cell lines and primary tissues

The PLC/PRF/5 (Alexander) human hepatoma cell line was obtained from the Japanese Collection of Research Bioresources (JCRB). HepG2.2.15 cells, kindly gifted by Professor Stephan Urban

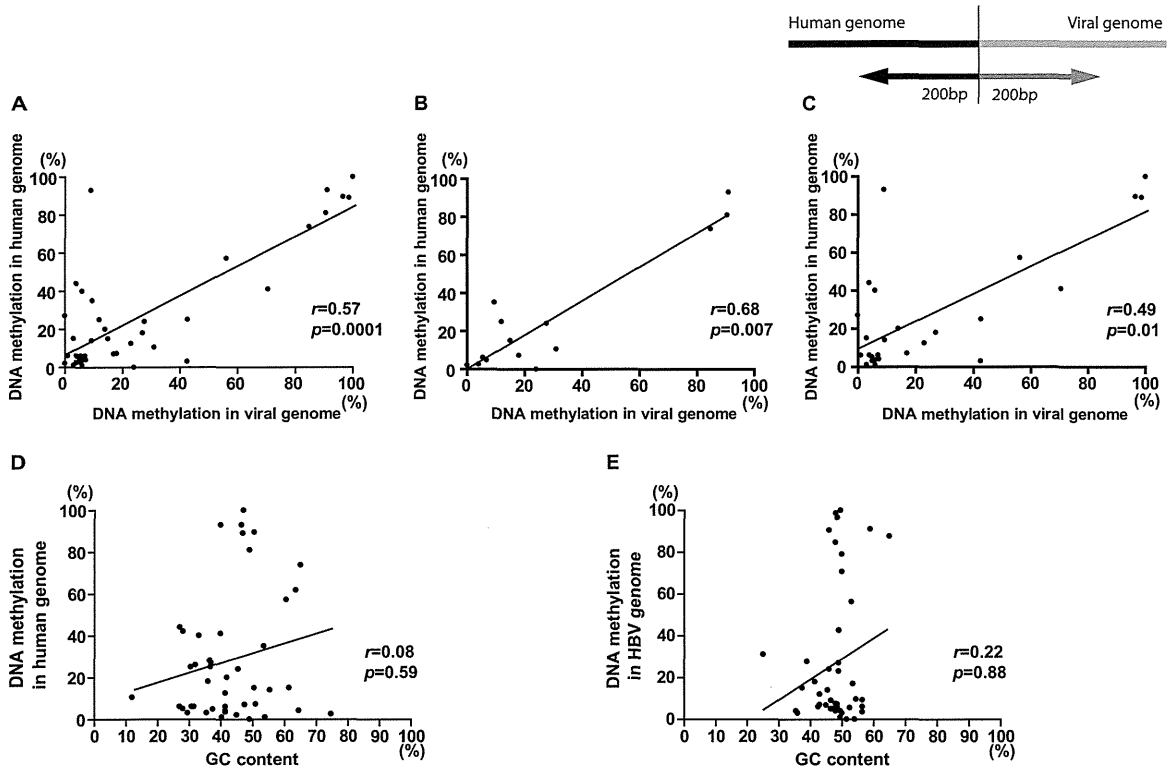

Figure 5. Correlation analysis between the methylation pattern of the integrated HBV DNA and that of the human genome. DNA fragments, including 200 bp of the HBV DNA and 200 bp of the human genome around the boundary, were analyzed for average methylation and GC content. (*A*) A correlation between the average methylation of the HBV DNA and that of the human genome in combined two cell lines and eight clinical samples ($n = 40$, $r = 0.57$, $P = 0.0001$, 95%CI = 0.3091–0.7545). (*B*) A correlation between the average methylation of the HBV DNA and that of the human genome in two cell lines ($n = 14$, $r = 068$, $P = 0.007$, 95%CI = 0.2233–0.8946). (*C*) A correlation between the average methylation of the HBV DNA and that of the human genome in eight clinical samples ($n = 26$, $r = 0.49$, $P = 0.01$, 95%CI = 0.1222–0.7463). (*D*) No correlation between the average methylation and GC contents in the human genome in the combined two cell lines and eight clinical samples ($n = 45$, $r = 0.08$, $P = 0.59$, 95%CI = −0.2253–0.3745). (*E*) No correlation between the average methylation and GC contents in the viral genome in the combined two cell lines and eight clinical samples ($n = 47$, $r = 0.22$, $P = 0.88$, 95%CI = −0.3151–0.2751).

at University Hospital Heidelberg, was derived from HepG2 cells transfected with a plasmid carrying four 5′-3′ tandem copies of the HBV genome (Koike et al. 1994). Cell lines were maintained in appropriate media containing 10% fetal bovine serum in plastic culture plates. Primary tissues from tumor and adjacent tissues were obtained at the time of the clinical procedures. Informed consent was obtained from all the patients before specimen collection. This study was approved by the institutional review board. DNA was extracted using the standard phenol–chloroform method. The concentration and quantity of extracted DNA were measured using a NanoDrop spectrophotometer (NanoDrop Technologies).

MCAM analysis

MCAM analysis was conducted as previously described (Oishi et al. 2012). A detailed protocol of MCA was previously described (Toyota et al. 1999). We used a custom human promoter array (G4426A-02212; Agilent Technologies) comprising 36,579 probes corresponding to 9021 unique genes. The probes on the array were selected to recognize SmaI/XmaI fragments mainly derived from sequences near gene transcription start sites. Five micrograms of genomic DNA was digested with 100 U of methylation-sensitive restriction endonuclease SmaI (New England Biolabs) for 24 h at 25°C, which cleaves unmethylated DNA leaving blunt ends (CCC/GGG). Subsequently, the DNA was digested with 20 U of methylation-insensitive restriction endonuclease XmaI for 6 h at 37°C, creating sticky ends (C/CCGGG). Five hundred milligrams of digested DNA was ligated using 50 μL of RMCA12 (5′-CCGGGCA GAAAG-3′)/RMCA24 (5′-CCACCGCCATCCGAGCCTTTCTGC-3′) primers and T4 DNA ligase (TaKaRa Bio) for 16 h at 16°C. After filling in the overhanging ends of the ligated DNA fragments at 72°C, the DNA was amplified for 5 min at 95°C followed by 25 cycles of 1-min incubation at 95°C and 3-min incubation at 77°C using 100 pmol of RMCA24 primer. MCA products were labeled with Cy5 (red) for DNA from hepatoma samples (both tumor and adjacent normal) and Cy3 (green) for DNA from human blood mixture of three healthy volunteers using a randomly primed Klenow polymerase reaction (Invitrogen) for 3 h at 37°C. Human CpG island arrays (4 × 44 K) were purchased from Agilent Technologies. Microarray protocols, including labeling, hybridization, and post-hybridization washing procedures, are provided at http://www.agilent.com/. Labeled samples were then hybridized to arrays in the presence of human Cot-1 DNA for 24 h at 65°C. After washing, arrays were scanned using an Agilent DNA microarray scanner and analyzed using Agilent Feature Extraction software (FE version 9.5.1.1, Agilent Technologies) at St. Marianna University School of Medicine. We used GeneSpring software (Agilent) for choosing candidate genes after normalization of the raw data.

DNA methylation analysis

Hidden Markov models have been successfully used to partition genomes into segments of comparable stochastic structure (Durbin et al. 1998). Using these models for sequence analysis performed

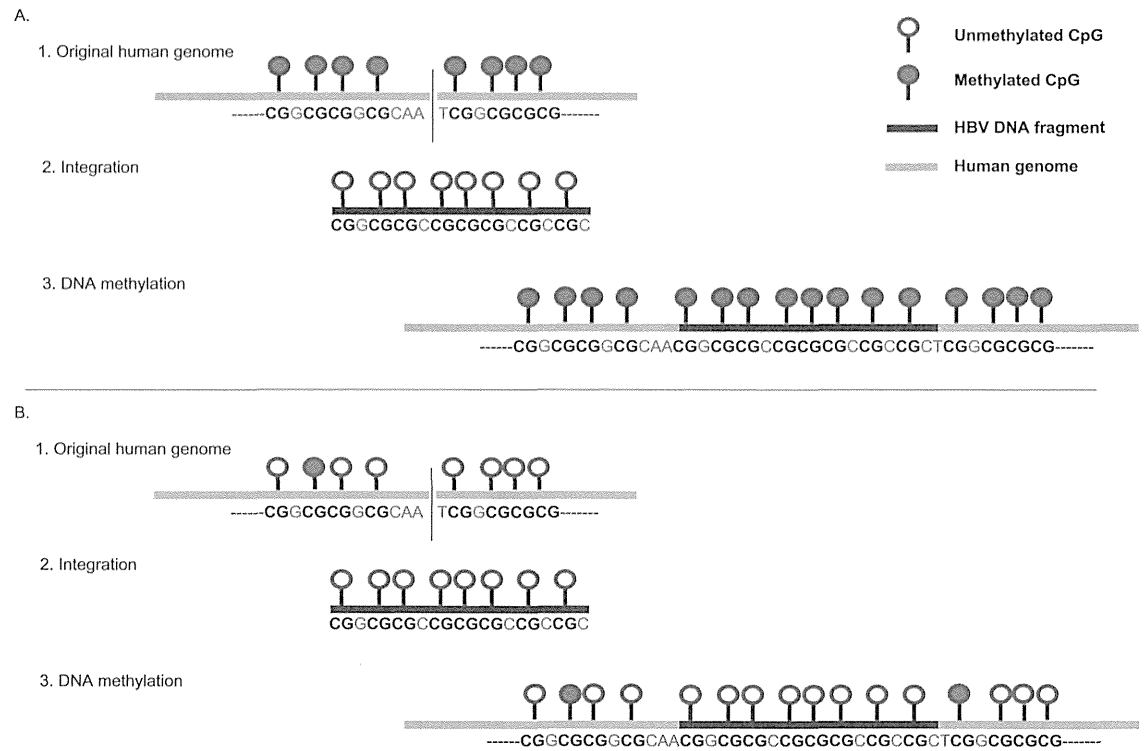

Figure 6. Schema of DNA methylation at HBV integrants and flanking human genomic sequences. (*A*) DNA hypermethylation was seen in both the integrated HBV fragment and human genome (original human genome shows dense methylation). The HBV genome often showed significant methylation when integrated into highly methylated host sites. (*B*) DNA hypermethylation was rarely seen in the integrated HBV fragment and human genome (original human genome shows low methylation). The HBV genome remained largely unmethylated when integrated into unmethylated host sites.

on the CpG plugin of bioinformatics software Geneious 5.5.8 (Biomatters), CpG islands were searched in the HBV genome (Kearse et al. 2012). Bisulfite PCR was performed using an EpiTect Bisulfite Kit (Qiagen) according to the manufacturer's protocol. One microliter of bisulfite-treated DNA was used as a template. The primers used for amplifying CpG sequences in the *HBx* gene are described in Supplemental Table 1. After PCR, the biotinylated strand was captured on streptavidin-coated beads (Amersham Bioscience) and incubated with sequencing primers (Supplemental Table 1). The pyrosequencing reactions were performed using the PyroMark Q24 and/or PyroMark Q24 advanced (Qiagen). Pyrosequencing quantitatively measures the methylation status of several CpG sites in a given sequence. These adjacent sites usually show highly concordant methylation. Therefore, the mean percentage of methylation at detected sites was used as a representative value for each sequence.

LINE1 and *Alu*Yb8 methylation analysis

The LINE1 and *Alu*Yb8 methylation levels, as measured by pyrosequencing, are good indicators of the cellular levels of 5-methylcytosine (i.e., the global DNA methylation level). To quantify relatively high LINE1 and *Alu*Yb8 methylation levels, we used pyrosequencing technology (Igarashi et al. 2010). PCR and subsequent pyrosequencing for LINE1 and *Alu*Yb8 were performed using the PyroMark kit (Qiagen). This assay amplifies a region of the LINE1 or *Alu*Yb8 elements that includes three CpG sites. The PCR was conducted as follows: 45 cycles for 20 sec at 95°C, for 20 sec at 50°C, and for 20 sec at 72°C, followed by 5 min at 72°C. The biotinylated PCR product was purified and converted to single strands to serve as a template for the pyrosequencing reaction using the pyrosequencing vacuum prep tool (Qiagen). The pyrosequencing reactions were performed using the PyroMark Q24 and/or PyroMark Q24 advanced (Qiagen). The percentage of Cs relative to the total sum of the Cs and Ts at each CpG site was calculated. The average of the percentages of Cs at the three CpG sites was used to represent the overall LINE1 and *Alu*Yb8 methylation levels in each sample.

FISH analysis of HBV integration

We developed a FISH analysis method to detect HBV DNA and demonstrate its presence in PLC/PRF/5 cells (Supplemental Fig. 3). The slides were pretreated with hydrogen peroxide and rinsed in 1× phosphate-buffered saline (PBS) to minimize background and quench endogenous peroxidase activity. To remove the excess cytoplasm, the slides were treated with pepsin and then fixed with 1% formaldehyde in PBS/$MgCl_2$. The slides were then dehydrated in an ethanol series (70%, 90%, and 100%) for 3 min at each step. The probes were designed based on the reference HBV sequence in PLC/PRF/5 DNA that is available from the Methylyzer 1.0 website (http://gbrowse.bioinfo.cnio.es/cgi-bin/VIRUS/HBV/). The FISH probes were prepared by combining the PCR-labeled probes (Supplemental Table 1), human Cot-1 DNA, and salmon sperm DNA. The probes were precipitated and mixed with hybridization buffer, and the probe DNA cocktail was denatured for 5 min at 95°C. The DNA on the slides was denatured by soaking in 70% formamide/2× SSC for 3 min at 74°C. The slides were immediately immersed in freshly prepared ice-cold 70% ethanol for 3 min, followed by 3-min immersions in 90% and then 100% ethanol. The denatured probe DNA was applied to the dry denatured slides and covered with a coverslip. The hybridization was performed for 16 h at 37°C.

Tyramide signal amplification (TSA)–FISH

TSA (tyramide signal amplification) detection kits were obtained from PerkinElmer. TSA-FISH detection was performed following the manufacturer's protocols with minor modifications. High stringency washes (0.1× SSC) were used to reduce the background, and TNT buffer (0.1 M Tris-HCl at pH 7.5, 0.15 M NaCl, 0.05% Tween 20) was adjusted to pH 7.0–7.5. The biotin- or DIG-labeled probes were detected using streptavidin-HRP or anti-DIG-HRP in TNB (0.1 M Tris-HCl at pH 7.5, 0.15 M NaCl, 0.05% blocking reagent [supplied in the kit]) for 30 min at room temperature and washed twice for 5 min each in TNT buffer. For the tyramide amplification procedure, the slide was covered with tyramide solution (Tyr-Bio, 1:50) for 10 min at room temperature. The tyramide solution was removed, and the slides were washed twice for 5 min each with TNT at room temperature. Fluorochrome-conjugated streptavidin (stAv-Alexa 488) diluted in TNB was used to detect the Tyr-Bio. The slides were incubated for 30 min at room temperature, washed with TNT buffer twice for 5 min each at room temperature, and covered with an anti-fade reagent containing DAPI (Speel et al. 1997; Schriml et al. 1999).

Identification of the chromosomal locations of viral–host junctions

The viral–host junctions were amplified using primers specific for human *Alu*Yb8 repetitive sequences and HBV X regions (Supplemental Table 1; Minami et al. 1995; Murakami et al. 2004). One microliter of genomic DNA solution served as a template in the subsequent PCR. We used touchdown PCR for most of the assays. All PCR assays included a denaturation step for 30 sec at 95°C, followed by an annealing step at various temperatures for 30 sec and an extension step for 30 sec at 72°C. PCR products were analyzed using electrophoresis through 1% agarose gels. PCR products were ligated to pCR-XL-TOPO vector DNA (TOPO XL PCR Cloning kit; Invitrogen) and transformed into competent cells. Positive colonies were selected and isolated using a QIA prep Spin Miniprep Kit (Qiagen). Direct sequence analysis of TOPO-TA cloning products was performed using a 3130 genetic analyzer (Applied Biosystems) (Watanabe et al. 2011). All sequences were searched for matches with HBV and pCR-XL-TOPO sequences using Geneious 5.5.8 (Biomatters) sequence analysis and assembly software and the BLAST program available on the UCSC Genome Browser (http://genome.ucsc.edu/).

Analysis of HBV DNA integration site sequences using NGS

Agilent's SureSelect target enrichment system is a highly efficient hybrid selection technique for optimizing NGS. We used this system and 12,391 custom baits covering the DNA sequences of HBV genotypes A to J and PLC/PRF/5 HBV sequences and optimized experiments for a GS FLX Titanium system (Roche). PLC/PRF/5, HepG2.2.15, and four paired tumor and nontumor samples (sample nos. 7, 8, 9, and 10 in Fig. 1B) were analyzed.

DNA methylation analysis of the integrated HBV genome as well as the adjacent human genome

DNA methylation was analyzed using bisulfite pyrosequencing (Oishi et al. 2012). The pyrosequencing reactions were performed using the PyroMark Q24 and/or PyroMark Q24 advanced (Qiagen). PLC/PRF/5, HepG2.2.15, and four paired tumor and nontumor samples (sample nos. 7, 8, 9, and 10 in Fig. 1B) were analyzed. Primers for methylation analysis of integration sites in PLC/PRF/5 are shown in Supplemental Table 1.

DNA methylation analysis of orthologous loci

Methylation levels of orthologous loci in HepG2.2.15 cells and in PBLs of a healthy volunteer at the same (empty) target sites of PLC/PRF/5 cells were analyzed using bisulfite pyrosequencing. Similarly, methylation levels of orthologous loci in PLC/PRF/5 cells and in PBLs at the same (empty) target sites of HepG2.2.15 cells were analyzed.

Allele-specific DNA methylation analysis of the integrated HBV genome as well as the adjacent human genome

Allele-specific DNA methylation was analyzed as described previously (Yamada and Ito 2011). The pyrosequencing reactions were performed using the PyroMark Q24 and/or PyroMark Q24 advanced (Qiagen).

Correlation analysis between the methylation pattern of the integrated HBV DNA and that of the human genome

DNA fragments, including 200 bp of the integrated HBV DNA and 200 bp of the human genome around the boundary, were analyzed for average methylation, GC content, and repetitive sequences in cell lines and clinical samples. RepeatMasker was used to identify repetitive elements in genomic sequences (AFA Smit, R Hubley, P Green, unpubl.). The Spearman correlation coefficient was used to assess correlations between the average methylation of the HBV DNA and that of the human genome. Correlations between GC content or repetitive sequences in the HBV DNA and the human genome were analyzed by using the Spearman correlation coefficient for continuous variables, and $P < 0.05$ was considered significant. All statistical analyses were performed using PRISM software for Windows, version 4 (GraphPad Prism).

Chromatin structure at the integrated HBV site

Using Bander software (Cheung et al. 2001; Furey and Haussler 2003), we analyzed the chromatin structure at the integrated HBV site in PLC/PRF/5 and HepG2.2.15.

Data access

All raw sequence data from this study have been submitted to the DDBJ Japanese Genotype-phenotype Archive (JGA; http://trace.ddbj.nig.ac.jp/jga/index_e.html) under accession number JGAS00000000015. Array data have been submitted to the NCBI Gene Expression Omnibus (GEO; http://www.ncbi.nlm.nih.gov/geo/) under accession number GSE59405.

Acknowledgments

We thank Drs. K. Watashi and T. Wakita for cell lines and Drs. T. Takayama, K. Takasaki, and S. Kawasaki for clinical samples. We also thank Drs. N. Matsumoto and N. Yamada-Ohkawa, as well as other members of the laboratory, for advice and suggestions. A part of the data used for this research was originally obtained by a research project of Hiroyuki Yamamoto and Yoshiyuki Watanabe led by Professor Fumio Itoh and is available at the website of the NBDC/JST (http://biosciencedbc.jp/en/). This work was supported in part by the Japan Society for the Promotion of Science (JSPS) Grants-in-Aid for Scientific Research (JSPS KAKENHI grant no. 23590964 to H. Yotsuyanagi).

Author contributions: Y.W. conceived the study, designed and performed the experiments, analyzed the data, and wrote the manuscript. H. Yamamoto designed the experiments, analyzed the data and wrote the manuscript. R.O. performed the experiments